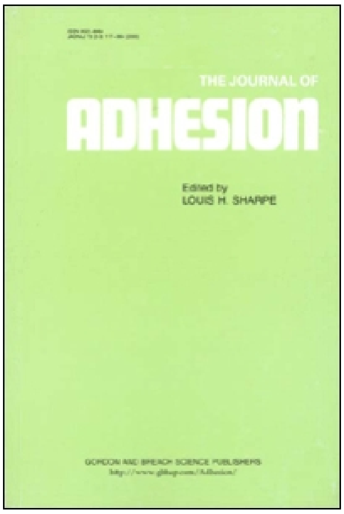

The Journal of Adhesion
Publication details, including instructions for authors and subscription information:
http://www.informaworld.com/smpp/title~content=t713453635

Two-Dimensional Interlaminar Stress Distribution within the Adhesive Layer of a Symmetrical Doubler Model

O. Ishai[a]; S. Gali[a]
[a] Faculty of Mechanical Engineering, Technion-Israel Institute of Technology, Haifa, Israel

To cite this Article Ishai, O. and Gali, S.(1977) 'Two-Dimensional Interlaminar Stress Distribution within the Adhesive Layer of a Symmetrical Doubler Model', The Journal of Adhesion, 8: 4, 301 — 312
To link to this Article: DOI: 10.1080/00218467708075092
URL: http://dx.doi.org/10.1080/00218467708075092

J. Adhesion, 1977, Vol. 8, pp. 301–312

Printed in Scotland

Two-Dimensional Interlaminar Stress Distribution within the Adhesive Layer of a Symmetrical Doubler Model

O. ISHAI and S. GALI

Faculty of Mechanical Engineering, Technion-Israel Institute of Technology, Haifa, Israel 32000

(*Received July 6, 1976*)

Two-dimensional stress distribution within the adhesive layer of a doubler model was derived by means of the finite element method. Results indicated significant variations in all stress components through the adhesive thickness in a region close to the adhesive edge, in contrast to the assumption of uniform stress distribution postulated by several authors. However, this assumption was found to be valid along most of the adhesive central length. The value, orientation and location of principal stresses, obtained by the analysis, may provide a guideline for the study of adhesive failure mechanism.

INTRODUCTION

In order to derive a closed form analytical solution for stress distribution within the adhesive of a single-lap-joint model, certain simplified assumptions were postulated by different authors,[1-5] namely: uniform shear and normal stress distribution through the thickness direction. The neglect of axial normal stress (σ_x) in the adhesive is also common to many publications on bonded lap joints.

Similar assumptions were made in a previous report[6] in order to obtain an analytical closed form solution for average stress distribution within the interlaminar adhesive layer (IAL) of a symmetrical doubler model (SMD). These simplifications, and the fact that the analytical model does not have sufficient degrees of freedom, lead to several inconsistencies in equilibrium relationships and violate the boundary condition of zero shear stress at the free IAL square edge.

Because of the mathematical complexity required of a more rigorous solution, and the fact that a realistic bond-line is very thin relative to adherend thickness, only a few studies have been made on IAL lateral stress distribution. Pirvics[7] obtained a solution by finite difference minimization of the internal energy distribution for typical lap and butt joint models. His solution, though suffering from inconsistencies, clearly indicates the pronounced non-uniformity in the distribution of both shear and normal stresses through the adhesive thickness.

Similar trends were found by Alwar and Nagaraja[8] who analyzed the butt-joint model by means of the finite element method (FEM).

The objective of the present study is to obtain a two-dimensional solution for stress distribution within the IAL of the doubler model by the same means. This will hopefully serve two purposes: to check available analytical solutions and to provide basic data for investigation of strength and failure of the system, for which the local principal stress components, rather than their average values, are required.

MODEL REPRESENTATION

IAL behavior is best represented by the SMD structural model shown in Figure 1. This model was also selected for the FEM program because of the following advantages:

— Double symmetry in geometry, materials, boundary, and loading conditions, which allows treatment of one quarter of the model only, and thus reduces the number of boundary conditions.

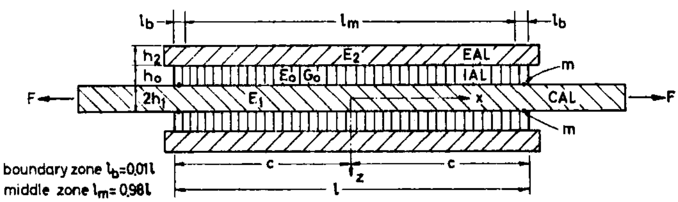

FIGURE 1 Symmetrical Doubler Model (SMD).

— Wide separation between external loading region and the critical IAL zones where maximum stresses and strains are located. This allows the isolation of the IAL boundary zone which is of main interest for both experimental and analytical study.

The model for the present specific case is composed of aluminum adherends and epoxy adhesive, the characteristics of which are given in Table I.

TABLE I

Characteristics of the SMD model

Elastic moduli [kg/mm²]				Dimensions [mm]			
G_0	E_0	E_1	E_2	h_0	h_1	h_2	c
90	250	7500	7500	1.0	1.5	1.0	65

The model for the finite element solution of the SMD is based on orthogonal and triangular elements with a uniform strain field. The elements satisfy the compatability conditions at each of the material points, as well as equilibrium conditions in each element. The mechanical behavior is limited to the elastic-linear range and to the two-dimensional case. A state of plane strain was assumed for the IAL (x–z plane) because of its high width-to-thickness ratio and its low adhesive-to-adherend stiffness ratio. Although this assumption is less accurate when relating to the adherend layers, it is justified for the present

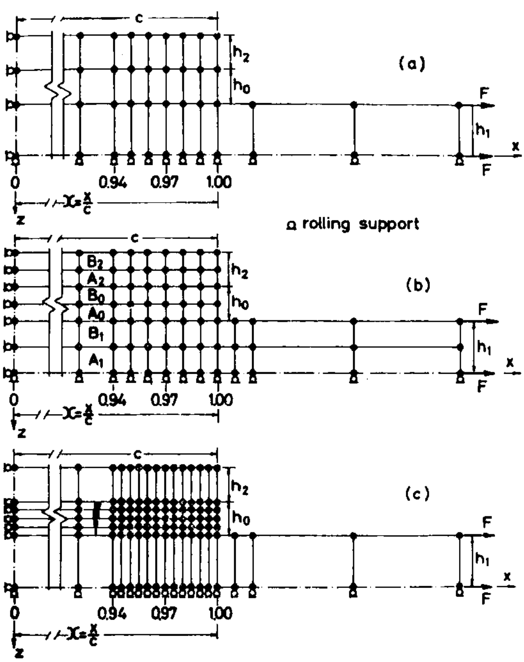

FIGURE 2 Illustration of the finite element networks for SMD for the three step program.

study which focuses on the IAL. The results of preliminary comparative studies between plane stress and plane strain conditions for the adhesive and adherends exhibited only small differences.

The FEM program consisted of three steps. In the first step, uniform stress distributions through IAL thickness was assumed and the IAL was divided into rectangular elements having the IAL lateral dimensions (Figure 2a).

In the second step, the IAL thickness was divided into two longitudinal strips (Figure 2b). In the final step, which aimed at deriving the stress distribution through the IAL thickness, it was divided into 4 longitudinal strips as shown in Figure 2c.

FEM VS. ANALYTICAL SOLUTION

The FEM was first examined by comparing its results (based on the model of Figure 2a) to the analytical closed-form solution of reference 6. Good agreement was found between numerical and analytical results both for the normal stress distribution (Figure 3) and for the shear stress distribution, except at the region close to the IAL edges (Figure 4).† A preliminary study of the effect of a finer network in the axial direction showed only slight

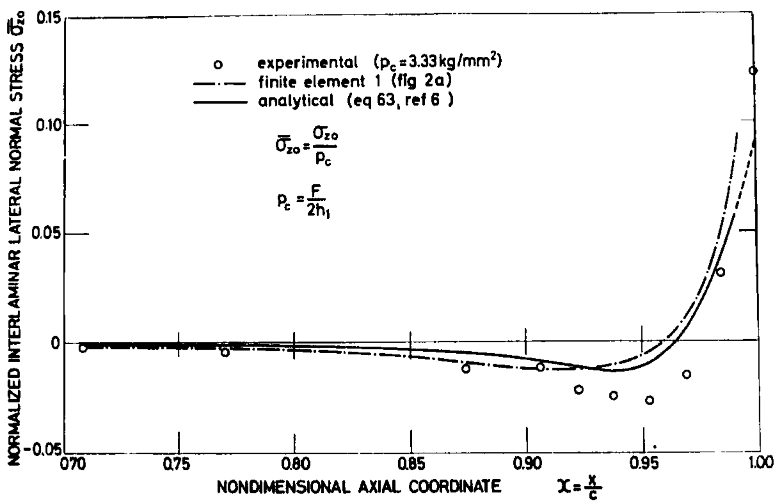

FIGURE 3 Axial distribution of IAL average lateral normal stresses (FEM versus analytical solution).

† In all stress distributions (Figures 3–11) the stresses are normalized with respect to average applied stress acting at the central adherend $p_c = F/2h_1$. Accordingly: $\bar{\tau}_{xzo} = \tau_{xzo}/p_c$; $\bar{\sigma}_{xo} = \sigma_{xo}/p_c$; $\bar{\sigma}_{zo} = \sigma_{zo}/p_c$.

differences in results. The FEM solution is also in agreement with experimental data which were obtained previously.[9]†

The second step revealed different stress patterns close to the edges. Shear stress distribution at the IAL external layer was found to reverse its

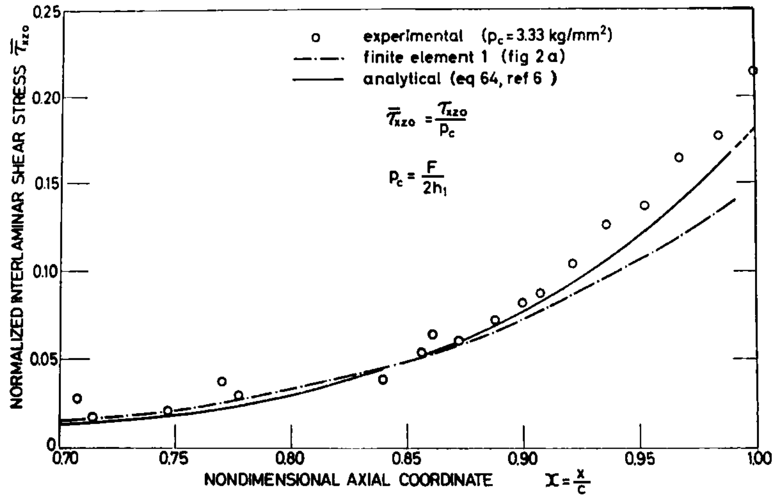

FIGURE 4 Axial distribution of IAL average shear stresses (FEM versus analytical solution and experimental data).

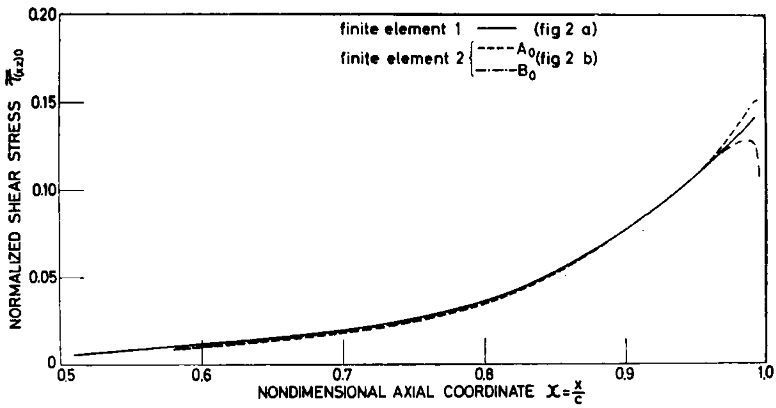

FIGURE 5 Axial distribution of shear stresses through the IAL (step 2).

† Shear and normal IAL displacements were measured by electromechanical extensometers.

slope at the boundary zone ($\chi > 0.98$) and to drop to zero towards the IAL edges (Figure 5). Normal stress, on the other hand, increased steeply towards the edge of the IAL layer close to the central adherend but reversed its slope and dropped steeply towards the free edges of the IAL layer close to the external adherend (Figure 6).

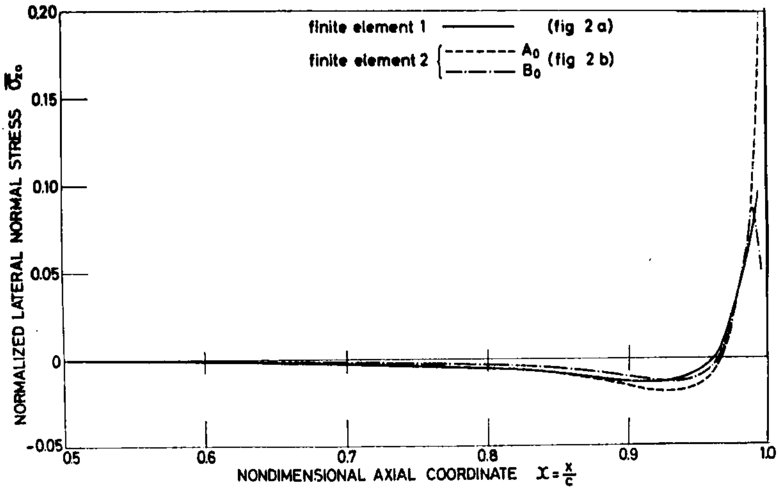

FIGURE 6 Axial distribution of lateral normal stresses through the IAL (step 2).

TWO-DIMENSIONAL STRESS DISTRIBUTION THROUGH ADHESIVE

The third step of the FEM solution in which the IAL was divided into 4 sub-layers (Figure 2) yielded the two-dimensional stress distributions.

In the IAL, all stress components are of the same order of magnitude and exhibited a pronounced variation through the thickness (along the z axis); (Figures 7–9).

The axial distribution of shear stress (τ_{xz0}) (Figures 8 and 5), showed a trend similar to that in Step 2, i.e., slope reversal at the "boundary zone" (from each edge up to a distance of 1% of the IAL length), and a drop towards zero at the free IAL edges. This finding is consistent with boundary conditions but contradicts the closed-form analytical solution.

Axial distribution of lateral normal stresses (σ_{z0}) along the "boundary zone" showed a pronounced divergence from their average reference distribution; whereas the normal stress through the internal IAL sublayer (I) rose steeply towards the edge far beyond its average level. The normal stress through the external sublayers (III, IV) reversed their slope at the "boundary zone" and dropped steeply towards the free edge (Figures 9 and 6).

Axial distribution of axial normal stresses (σ_{x0}) was uniform throughout the "middle zone" (98 % of the IAL length) but dropped within the "boundary zone" towards zero at the free edges (Figure 7).

It may be concluded that axial interlaminar stress distributions (σ_{z0}, τ_{xz0}) derived by FEM are in close agreement with the closed-form solutions along the "middle zone". The major divergence between the numerical and closed-form solutions resulted from the assumption of uniform lateral stress distributions. As shown in Figures 8 and 9, such an assumption did not hold up at the "boundary zone" in cases of shear and normal lateral stresses.

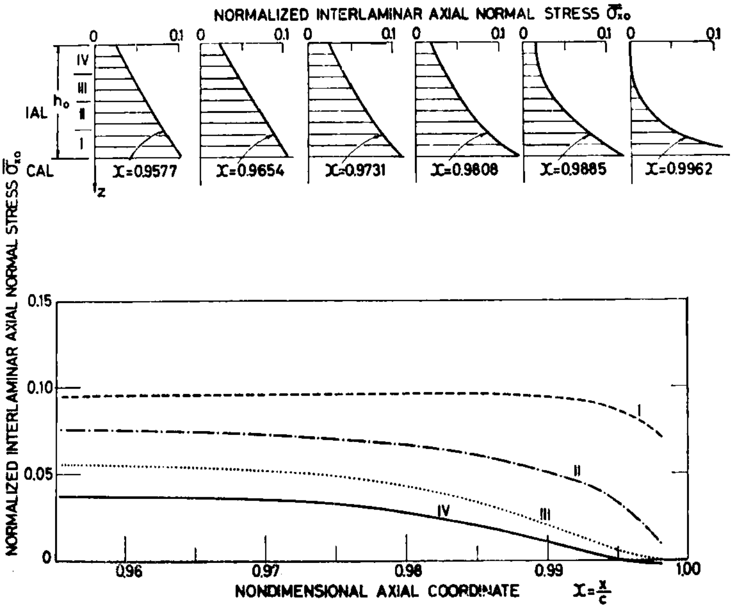

FIGURE 7 Distributions of axial normal stresses close to the IAL edges (step 3).

The neglect of axial normal stresses through the IAL is also unjustified as these stresses attained a level having the same order of magnitude as other stress components (Figure 7).

Lateral normal stress distribution at the boundary zone shows the maximum deviation from uniformity (Figure 9) being almost zero close to the external adherend and increasing steeply and linearily to its maximum level towards the central adherend. Similarly, both IAL shear and axial normal stresses attained their maximum value close to the intersection of the free IAL edge and the upper surface of the central adherend (point *m* of Figure 1).

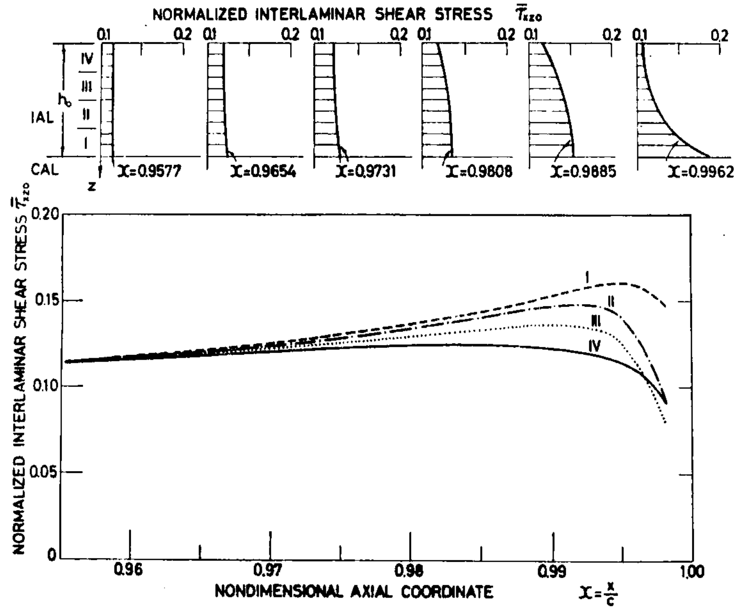

FIGURE 8 Distributions of shear stresses close to the IAL edges (step 3).

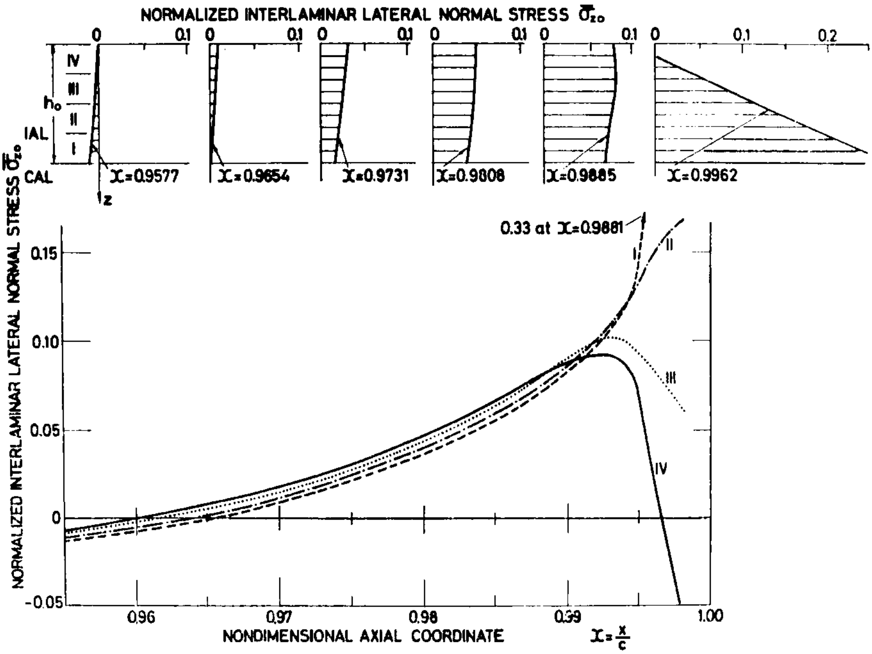

FIGURE 9 Distributions of lateral normal stresses close to the IAL edges (step 3).

DISCUSSION

Given the values of the three stress components at the IAL boundary zone, their principal value can be derived. Figures 10 and 11 show the axial and lateral distributions of the principal stresses and their orientation, emphasizing the major trends found for the stress components. The expected finding of the location of maximum stress being close to point *m* is also demonstrated.

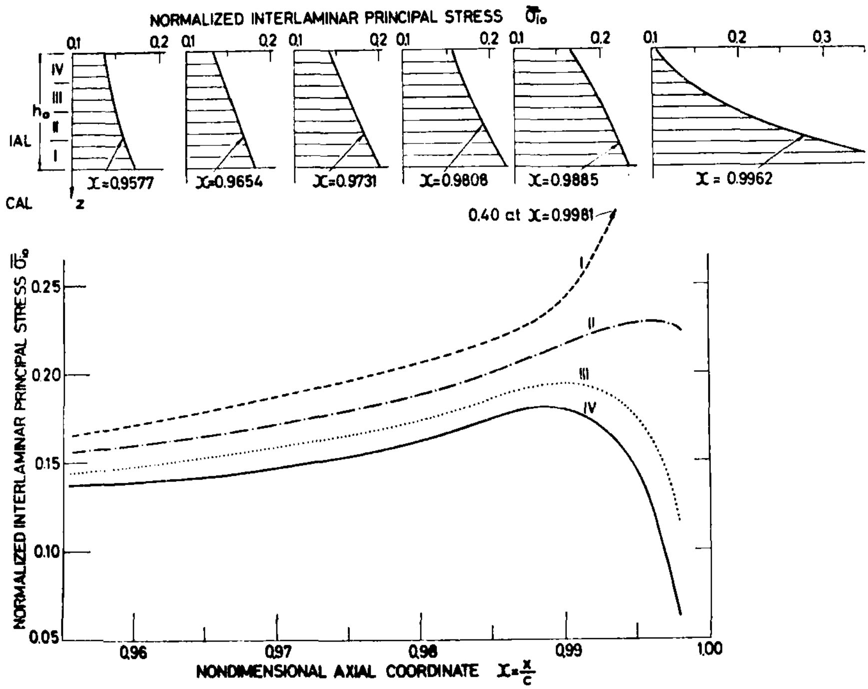

FIGURE 10 Distributions of principal stresses close to the IAL edges.

In the case of brittle IAL characteristics, the data given by the principal stress distribution may provide the basic clue for failure mechanism, the delamination process, and strength evaluation for the overall bonded structure as represented by the SMD model. The finite element method seems to provide an accurate solution which conforms well to basic mechanical and boundary conditions and successfully sensed the singularities that exist at the bond-line edge. The interrelation among the different functions found for the different stresses can be examined by satisfying the classical equilibrium conditions.

According to the first equilibrium equation,

$$\frac{\partial \sigma_x}{\partial x} = -\frac{\partial \tau_{xz}}{\partial z} \tag{1}$$

which means that τ_{xz} is uniformly distributed along the z axis in the region where σ_x is uniformly distributed along x. This interrelation prevails at the "middle zone" of the IAL, as is shown when Figure 8 is compared with Figure 7.

According to the second equilibrium equation,

$$\frac{\partial \sigma_z}{\partial z} = -\frac{\partial \tau_{xz}}{\partial x} \tag{2}$$

which means that where the τ_{xz} distribution along x reverses its slope, the σ_z function along z will also reverse but in the opposite direction. This change occurs simultaneously for the two functions at about $\chi = 0.994$ within the "boundary zone", as demonstrated by a comparison of Figure 8 with Figure 9.

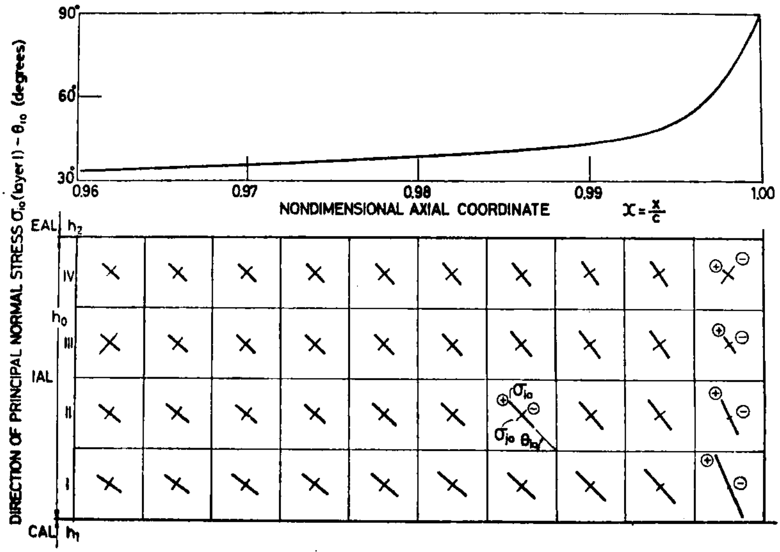

FIGURE 11 Variation of principal stresses orientation through the IAL (sublayer I, figure 2c).

At the middle zone, the $\tau_{xz}(x)$ functions coincided (Figure 8), thus σ_z functions are supposed to be linear functions of z, as is evident from Figure 9.

The above findings referred to an idealized case of thick adhesive relative to its adherends. It is expected that similar distribution patterns will be found, though to a lesser degree, for the more practical cases of thinner and stiffer adhesives. The effect of changes in model geometry and stiffness ratio on

IAL stresses, which is relevant to the analysis and design of structural adhesive joints, may easily be derived by the present FEM program. Results of such study, which is beyond the scope of the present paper, will be published in the near future. The most important finding of the locations of the maximum principal stresses is also expected to be generally valid in the case of structural adhesives.

A more detailed solution for interlaminar adherend stresses is essential for the strength analysis of orthotropic composite bonded systems.

In order to obtain more realistic solutions which provide quantitative data for design allowables, the effects of nonlinearity in an adhesive stress-strain relationship and the effect of edge geometry have to be studied.

Some of the above topics are currently being treated by the finite element method and will be presented in the future.

CONCLUSIONS

The following conclusions emanate from the solutions obtained by applying the finite element method to a symmetrical doubler model, composed of aluminum adherends bonded by thick adhesive layers (IAL). Most of the conclusions concern distributions through the IAL, which is the main subject of the present investigation.

1) The distribution of shear and lateral normal stresses through the IAL thickness was approximately uniform within the "middle zone" ($-0.98 < \chi < 0.98$).

2) Axial normal stress distribution [$\sigma_x(x, z)$] was uniform within the "middle zone" but varied linearly through the IAL thickness.

3) For all interlaminar stress functions, drastic variations occurred at the "boundary zone" ($-0.98 > \chi > 0.98$).

4) The axial distribution of IAL shear stress attained its maxima within the "boundary zone", reversed its slope and dropped towards zero at the free edge. A similar trend was found for σ_z distribution close to the external adherends.

5) The normal lateral stress functions $\sigma_z(z)$ exhibited an approximately linear distribution which reversed its slope abruptly within the "boundary zone".

6) Maximum values of all stresses and their principal counterparts were attained at the "boundary zone", close to the central adherend interface.

7) The different patterns which characterized stress functions along the z and x axes were consistent with basic differential equilibrium equations and boundary conditions of the IAL.

8) The average interlaminar stress levels were significantly lower than their actual individual extreme levels; thus, they could not be used to predict the doubler strength.

9) Because of the narrow dimensions of the boundary zone, its stress behavior will not be reflected in the overly deformational behavior of the bonded structure, nor could this behavior be directly detected experimentally. It is, however, predominantly influential on the ultimate behavior of the IAL and has to be considered when failure mechanism and strength characteristics are discussed.

Acknowledgement

The present publication is part of a research project sponsored by the European Research Office, U.S. Army, under Contract No. DAJA 37-75-C-1890.

References

1. M. Goland and E. Reissner, *J. Appl. Mechanics* **11,** A17 (1944).
2. R. W. Cornell, *J. Appl. Mechanics* **20,** 355 (1953).
3. E. W. Kuenzi and G. H. Stevens, "Determinator of the Mechanical Properties of Adhesives for Use in the Design of Bonded Joints", US-FPL Report FPL-011 (1963).
4. O. Volkersen, *Construction Métalliane* **4,** 3 (1965).
5. W. J. Renton and J. R. Vinson, "The Analysis and Design of Composite Material Bonded Joints under Static and Fatigue Loadings", AFOSR=1760-72, Scientific Report AFOSR-TR-73-1627 (1973).
6. O. Ishai, D. Peretz and N. Galili, "Mechanical Behavior of Multiphase Composite Systems", Final Technical Report, Contract No. DAJA-37-74-C-2531; Technion–Israel Institute of Technology, TDM 73-11 (1973).
7. J. Pirvics, *J. Adhesion* **6,** 207 (1974).
8. R. S. Alwar and Y. R. Nagaraja, *J. Adhesion* **7,** 279 (1976).
9. O. Ishai, D. Peretz and S. Gali, "Direct Determination of Interlaminar Stresses in Polymeric Adhesive Layer", First Quarterly Status Report, European Research Office, U.S. Army, Contract No. DAJA 37-75-C-1890 (1975). (To be published in the Journal of the Society for Experimental Stress Analysis.)